FEBS Letters 373 (1995) 262–264 FEBS 16130

Electron cryomicroscopy of two-dimensional crystals of the H^+-ATPase from chloroplasts

Bettina Böttcher[a,b], Peter Gräber[b,*], Egbert J. Boekema[c], Uwe Lücken[a,**]

[a]*Fritz-Haber Institut, Faradayweg 4–6, D 14195 Berlin, Germany*
[b]*Institut für Physikalische Chemie, Universität Freiburg, Albertstr. 23a, D-79104 Freiburg, Germany*
[c]*Biofysische Chemie, Rijksuniversiteit Groningen, Groningen, The Netherlands*

Received 1 September 1995

Abstract The H^+-ATPase from spinach chloroplasts was isolated and purified. Two-dimensional crystals were obtained from the protein/lipid/detergent micelles by treatment with phospholipase and simultaneous removal of detergent and fatty acids by Biobeads. The resulting two-dimensionally ordered arrays were investigated by electron cryomicroscopy. The ordered arrays showed top view projections of CF_0F_1. The images were analysed by correlation averaging. In this view CF_0F_1 has dimensions of 11.4×9 nm. The average view shows a strongly asymmetric molecule, in contrast to the rather hexagonal features of CF_1, previously analyzed from two-dimensional arrays. It is concluded that this is due either to an asymmetric structure and positioning of CF_0 relative to CF_1 or to a rearrangement of CF_1 subunits induced by binding of CF_0 to CF_1.

Key words: Chloroplast; H^+-ATPase; Two-dimensional crystal; Electron cryomicroscopy

1. Introduction

Membrane-bound H^+-ATPases catalyze ATP synthesis and ATP hydrolysis coupled with a transmembrane proton transport in bacteria, chloroplasts and mitochondria. These enzymes have a hydrophilic part, F_1, containing the nucleotide binding sites and a membrane integrated part, F_0, which is involved in proton transport. The structure of the F_1-part from mitochondria was reported recently with a resolution of 2.8 Å [1]. In chloroplasts the CF_1-part has five different subunits with the stoichiometry $\alpha_3\beta_3\gamma\delta\varepsilon$ [2,3], the CF_0-part has four subunits [4] and has presumably the stoichiometry I II III_{12} IV [5].

The structure of the isolated holoenzyme was investigated by electron microscopy with negatively stained samples [6–8] and after embedding of the enzyme in amorphous ice, i.e. samples were frozen rapidly and electron micrographs were taken at about −171°C [9–11]. It was found that the side view projection of F_0F_1 had a tripartite structure: the hydrophilic F_1-part was connected to the hydrophobic F_0-part by a thin stalk.

Embedding biological macromolecules in thin layers of amorphous ice and imaging them by electron microscopy at liquid nitrogen temperature guarantees that the macromolecules are directly imaged in a form as close to the native state as possible. Full ATP synthesis after freezing and thawing was demonstrated for reconstituted CF_0F_1 [11]. The thin layer of ice gives the molecules a relatively large number of possibilities to be oriented. Image processing of the different orientations is difficult due to the low signal-to-noise ratio, finding the proper orientation and combining only particles which have the same orientation even more. The difficulties increase with decreasing molecular mass but can be circumvented substantially if proteins can be ordered in two-dimensional crystals or two-dimensional arrays. The arrays restrict the number of possible orientations, which facilitates the analysis considerably. The size and packing quality of the crystals determine the resolution that can be obtained. For large arrays (over 5 μm diameter) of small proteins atomic resolution has been obtained in two cases [12,13]. Recently, the analysis of negatively stained two-dimensional crystals of mitochondrial H^+-ATPase has been reported [14]. In this work, we have investigated two-dimensional crystals of CF_0F_1 by electron cryomicroscopy using image analysis for improvement of the signal to noise ratio.

2. Materials and methods

CF_0F_1 was prepared as described earlier [5]. The enzyme was stored in liquid nitrogen in a medium containing 40% saccharose, 40 mM Tris-succinate (pH 6.5), 0.5 mM EDTA, 0.2 mM ATP, 2 g/l Triton X-100 and 1 g/l asolectin. For very high protein to lipid ratios the CF_0F_1 preparation was dialyzed without any addition of detergent or lipid. If necessary, these samples were diluted to a final concentration of 1.5–6 g/l lipid with buffer (10 mM Na-tricine pH 8.0, 2.5 mM $MgCl_2$, 0.25 mM dithiothreitol, 0.2 mM ethylendiamintetraacetic acid).

For crystallization 100 mM $CaCl_2$ was added to aliquots of 20 μl sample. The sample was then treated with 10–100 U/ml phospholipase A2 and about 5–20 Bio-beads (SM7 Biorad) for up to 14 days at 4°C. The ordering process was monitored by electron microscopy using negatively stained samples. The advance of crystallization was controlled as follows: a sample was diluted 1:20 to 1:50 in water and immediately applied onto a carbon-coated 400 mesh copper grid. The sample was briefly washed twice with 1% uranylacetate and then stained for about 1 min with 1% uranylacetate. Electron microscopy was performed with a Philips EM 300 operating at 80 kV. Samples which showed a large proportion of ordered arrays were used for electron cryomicroscopy.

For electron cryomicroscopy holey carbon coated 400 mesh copper grids were used. The grids were glow discharged in air for about 45 s and then used for the freezing experiment within one hour. Cryomicroscopy was performed according to [15]. For freezing 2–3 μl sample (in some cases diluted 1:1 with water) were applied onto the grid already mounted in the freezing device. Excess sample was removed by pressing a filter paper (Whatman No. 1) for about 5 s against either the side where the sample was applied to or against the other side. Immediately after blotting the grid was plunged into liquid ethane cooled with liquid nitrogen with a guillotine-like device. Frozen grids were handled under liquid nitrogen and stored up to several weeks in liquid nitrogen. Microscopy was done using a DEEKO 200 or a Philips CM12 microscope operating at 100 kV. A Gatan cryostage was used in the CM12. Search-

*Corresponding author. Fax: (49) (761) 203 6189.

***Present address:* Philips Elektron Optics, PO Box 218, 5600 MD Eindhoven, The Netherlands.

SSDI 0014-5793(95)01058-0

ing for useful arrays was carried out at 5000× magnification using a TV set in order to minimize preexposure. Images of suitable areas were recorded on Kodak SO163 film under low-dose conditions at 40,000× (approx. 400–500 e/nm^2) or 60,000× (approx. 960–1300 e/nm^2) magnification with a defocussing value between 0.7–2 μm underfocus.

Micrographs were scanned with a Datacopy Model 610 F with a scanstep of 25 μm. Image processing was carried out using the IMAGIC software package [16]. Images from ordered arrays were analysed by correlation averaging [17]. Arrays were divided into small fragments with a side length of about 40.8 nm and a CF_0F_1 in the center surrounded by the next nearest molecules. The small fragments were overlapping but each time another F_0F_1-ATPase was centered in the fragments. The data set of these images was normalized in its grey value distribution and masked with a circular mask of a radius of 20.4 nm. The data set was aligned to one of its images as reference. Alignment was done in two consecutive steps, doing first the translational alignment and then in a second step an additional rotational alignment. Rotation in the rotational alignment was restricted to 10°. The images showing the highest cross-correlation coefficient were summed and the sum was used as a new reference for alignment. This process was repeated until no further improvement could be observed.

3 Results and discussion

We tried to crystallize CF_0F_1 starting with mixtures of CF_0F_1, lipid and detergent by optimizing protein-to-lipid ratios and other parameters. Ordered arrays of CF_0F_1 were produced by treatment with phospholipase A_2 and Biobeads. About 48 h after starting the treatment the first ordered arrays appeared. The packing quality and quantity of the arrays improved in time and was in most cases optimal after 5–7 days. The size of the arrays depended on the $CaCl_2$ concentration. At low concentrations (0–10 mM $CaCl_2$ the arrays grew larger, but they were less frequent and sometimes no ordered array was detected. At higher $CaCl_2$ concentration (100 mM) the ordered arrays were smaller but occurred more frequently.

In the negatively stained samples the arrays showed two types of arrangements. In some arrays the molecules were hexagonally packed and in others they seemed to be more densely packed in one direction and so that the arrays had a more striated appearance. Both types of arrays were much stronger stained than CF_1-crystals obtained under the same conditions [18].

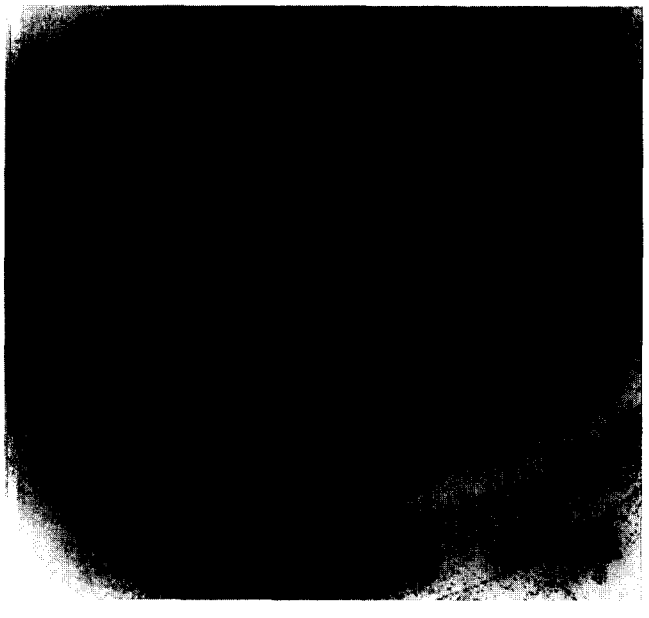

Fig. 1. Electron micrograph of an ordered two-dimensional array of CF_0F_1 in amorphous ice.

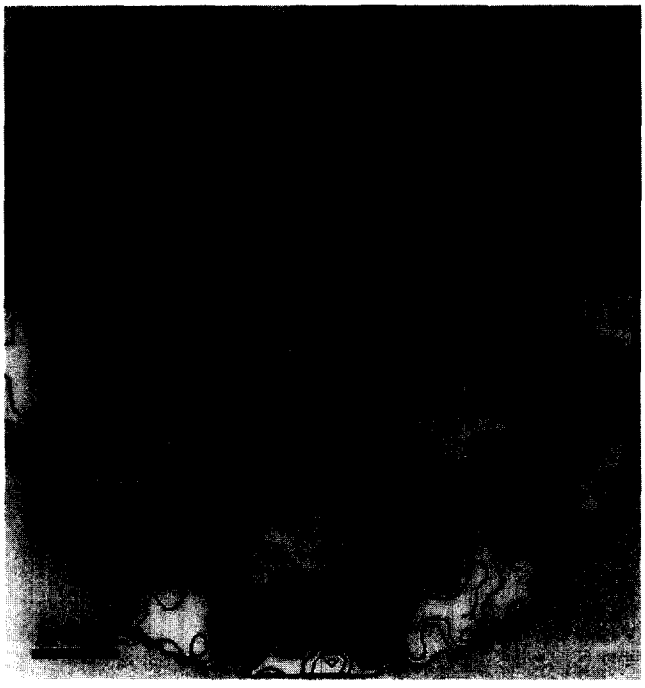

Fig. 2. Top view projection of CF_0F_1 in a two-dimensional array. Data from 30 fragments from an ordered array are oriented and averaged. Details see text.

When such samples were embedded in amorphous ice, the same types of arrays could be observed. Fig. 1 shows an example of such an ordered array. Though the appearance of the arrays varied, the periodicity of the lattice was always about 11.3 nm. For image processing by correlation averaging such an array was divided into a set of small fragments. The size of the fragments was chosen such that seven complete molecules were present surrounded by parts of the neighbour molecules. As the first reference one fragment of the data set was used. No additional mask was applied, so that the fragments aligned not just to one molecule but rather to several ones. In this way the influence of individual properties of the first reference was widely reduced. Since the arrays were rather small the number of fragments in each data set was limited to about 50–100. It was avoided to merge data from different arrays because of the different appearance of the lattices. Fig. 2 shows the result of this averaging procedure for a representative array. The average image shows the molecule in the center clearly, but the details of the surrounding particles are blurred, what would be expected if the arrays were not highly ordered. In the arrays with the hexagonal appearance the molecules have a blobby shape with a little tail sticking out at one end. All molecules in the arrays selected for processing are oriented in the same way. No symmetry elements were observed. This results in a P1 type of symmetry for the crystal packing.

Beside the two-dimensionally ordered arrays also string like structures are seen in Fig. 1. These strings can be interpreted as one-dimensionally packed CF_0F_1 molecules. The F_0-parts are in the center of the string, presumably with some lipids between them, still maintaining the structure of a lipid bilayer.

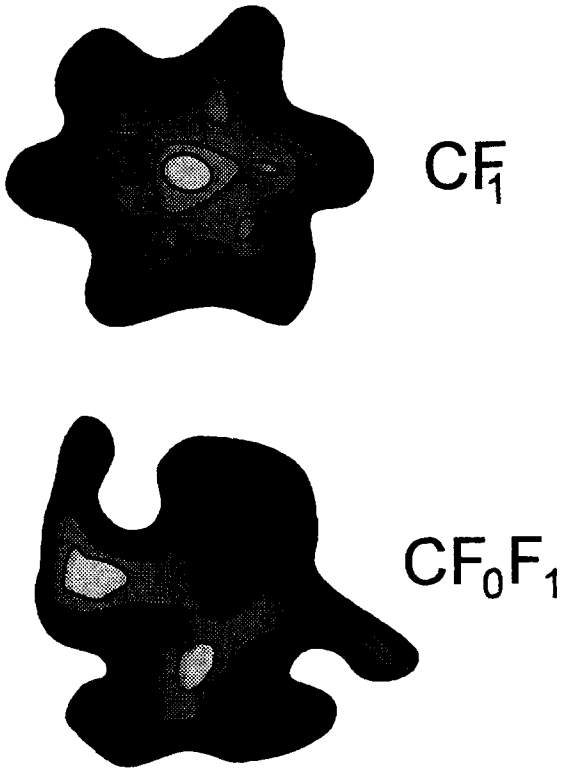

Fig. 3. Top view projections from two-dimensional crystals. Top: average image of CF_1 from negatively stained two-dimensional crystals (data from [18]). Bottom: average image of CF_0F_1 from two-dimensional arrays embedded in amorphous ice (from fig. 2).

The F_1-parts are sticking out to both sides, connected by a stalk. If these strings would be arranged into a two-dimensional crystal and seen in the top view, it would be expected that one half of the molecules are related to the other half via a mirror operation. The hexagonal packed arrays show no screw axis (see Fig. 2). This means that all molecules are pointing in the same direction. In the strings the F_1-parts are almost touching despite only every second molecule is oriented in the same direction. Nevertheless, the F_0-parts in the strings still have enough space. Since in the ordered arrays all molecules are oriented in the same direction, there must be plenty of space between the F_0-parts. Thus, it is likely that for the interaction between the molecules the F_1-parts are making the major contribution. It should be mentioned that the lattice repeat in the two-dimensional CF_1-crystals is 11 nm and this is similar to that of the two-dimensional CF_0F_1 arrays (11.3 nm).

The image shown in Fig. 2 is a projection through the holoenzyme and it is, therefore, not possible to say which part of the density in the average image results from which subunit. However, we can compare the average image from negatively stained two-dimensional CF_1 crystals with that of the CF_0F_1 crystals. Fig. 3 top shows an average image of the top view of CF_1 crystals. Fig. 3 bottom shows the same view of CF_0F_1 (from Fig. 2). It is evident that CF_1 appears to be rather 6-fold symmetric and that the attachment of CF_0 leads to a strong asymmetry of the molecule. This might be due either to a rearrangement of the α- and β-subunits when CF_0 is attached to CF_1, or it reflects the asymmetric positioning and structure of CF_0 since Figs. 2 and 3 show the projected density through the holoenzyme. Possibly, both effects might play a role.

It should be mentioned that the two-dimensional crystals of mitochondrial MF_0F_1 have a different appearance: presumably the MF_1-parts are directed alternatingly to different sides of the crystal. The hexogonal arrangement of the large subunits known from MF_1 can also be observed in MF_0F_1, however, also in this case an asymmetry can be seen.

Acknowledgements: This work was supported by a grant of the European Union BIO-CT93-0078.

References

[1] Abrahams, J.P., Leslie, A.G.W., Lutter, R. and Walker, J.E. (1994) Nature 370, 621–628.
[2] Süß, K.H. and Schmidt, O. (1982) FEBS Lett. 114, 213–217.
[3] Moroney, J.V., Lopresta, L., McEwer, B.F., McCarty, R.E. and Hammes, G.G. (1983) FEBS Lett. 158, 58–62.
[4] Fromme, P., Gräber, P. and Salnikov, J. (1987) FEBS Lett. 218, 27–30.
[5] Fromme, P., Boekema, E. and Gräber, P. (1987) Z. Naturforsch. 42c, 1239–1245.
[6] Soper, J.W., Decker, G.L. and Pedersen, P.L. (1979) J. Biol. Chem. 254, 11170–11176.
[7] Boekema, E., Schmidt, G., Gräber, P. and Berden, J.A. (1988) Z. Naturforsch. 43c, 219–225.
[8] Tsuprun, V.L., Mesyanzhinova, J.V. and Orlova, E.V. (1989) FEBS Lett. 244, 279–282.
[9] Gogol, E.P., Lücken, U. and Capaldi, R.A. (1987) FEBS Lett. 219, 274–278.
[10] Lücken, U., Gogol, E.P. and Capaldi, R.A. (1990) Biochemistry 29, 5339–5343.
[11] Böttcher, B., Lücken, U. and Gräber, P. (1995) Biochem. Soc. Trans. (in press).
[12] Henderson, R., Baldwin, J.M., Ceska, T.A., Zemlin, F., Beckmann, E. and Downing, K.H. (1990) J. Mol. Biol. 213, 899–920.
[13] Kühlbrandt, W., Wang, D.N. and Fujiyoshi, Y. (1994) Nature 367, 614–621.
[14] Dubachev, G.E., Lunev, A.V., Barnakov, A.N., Belogrudov, G.I., Grinkevich, V.A. and Demin, V.V. (1993) FEBS Lett. 336, 181–183.
[15] Dubochet, J., Adrian, M., Chan, J.-J., Homo, J.-C., Lepault, J., McDowell, A.W. and Schultz, P. (1988) Q. Rev. Biophys. 21, 129–228.
[16] van Heel, M. and Frank, J. (1981) Ultramicroscopy 6, 187–194.
[17] Saxton, W.O. and Baumeister, W. (1982) J. Microsc. 127, 127–138.
[18] Boekema, E., Schmidt, G., Gräber, P. and Berden, J.A. (1988) Z. Naturforsch. 43c, 219–225.